The Eurasia Proceedings of Science, Technology, Engineering & Mathematics (EPSTEM)
ISSN: 2602-3199

The Eurasia Proceedings of Science, Technology, Engineering & Mathematics (EPSTEM), 2024

Volume 32, Pages 123-130

IConTES 2024: International Conference on Technology, Engineering and Science

Comprehensive Investigation of Structural, Electronic and Optical Properties of KBaP Using Density Functional Theory

Aidouni Ahmed Amine
University of Ahmed Draya, Adrar

Ould-Mohamed Mounir
University of Blida

Aissat Abdelkader
University of Ahmed Draya, Adrar

Belbachir Souheil
University Abdelhamid Bn Badis of Mostaganem

Abstract: In this study, we investigate the structural, mechanical, dynamical, electronic, thermodynamic, and optical properties of KBaP using density functional theory (DFT) within the plane-wave pseudopotential method as implemented in Quantum ESPRESSO. Our structural analysis reveals that the β-phase of the half-Heusler structure is the most stable, with an equilibrium lattice parameter of 7.36 Å. Mechanical and dynamical stability are confirmed through the calculation of elastic constants and phonon dispersion, respectively. Electronic properties show that KBaP is a direct bandgap semiconductor with a bandgap of 1.30 eV at the X-X point, suggesting potential applications in optoelectronic devices. Additionally, we explore the thermodynamic and optical properties, further demonstrating the potential of KBaP in energy-related applications. Our findings provide a comprehensive understanding of KBaP, establishing it as a promising material for future technological developments.

Keywords: Half Heusler alloys, Electronic properties, Optical properties, Phonon dispersion curves

Introduction

Heusler compounds, discovered by Friedrich Heusler in the early 20th century, are recognized for unique properties such as the ferromagnetism of Cu_2MnAl, despite comprising non-magnetic elements (Heusler, 1903). Over 1000 compounds exist, categorized as full-Heusler and half-Heusler based on valence electron count, with applications in solar cells and spintronics (Wederni et al., 2024; Felser & Hirohata, 2015; Hayashi et al., 2020; Tavares et al., 2023; Graf et al., 2016).

Full-Heusler (X_2YZ) and half-Heusler (XYZ) compounds crystallize in $L2_1$ (space group 225, Fm-3m) and C1b (space group 216, F-43m) structures, respectively, with the latter containing transition metals at X and Y sites and a main group element at Z (Felser & Hirohata, 2016). The electronic properties vary, with 8-valence electron systems acting as semiconductors and 18-electron systems exhibiting tunable band gaps (0 to 4 eV) based on electronegativity differences. These features have driven significant research in spintronics and topological insulators. Certain half-Heusler compounds, like KBaP, are underexplored. DFT studies report a lattice parameter of 7.65 Å (Gruhn, 2010) And 7.36 Å (Carrete et al., 2014). Suggesting a foundation for future research. (Zhang et al., 2012). Found an indirect band gap of 2.03 eV for KBaP using DFT and the GW approximation.

This study explores KBaP, a stable half-Heusler compound notable for its dynamic, mechanical, electronic, thermal, and optical properties. Despite previous research, many of its physical characteristics remain underexamined, necessitating a thorough investigation. Utilizing advanced techniques such as DFT (Hohenberg & Kohn, 1964; Kohn & Sham, 1965). And density functional perturbation theory (DFPT) (Baroni et al., 2001a). We analyzed its lattice, elastic, electronic, and optical properties, aiming to enhance understanding of KBaP and evaluate its potential for thermoelectric and optoelectronic applications.

Computational Methodology

This study employed first-principles calculations using density functional theory (DFT) and the pseudopotential plane-wave method in Quantum Espresso (QE) (Giannozzi et al., 2017; Giannozzi et al., 2020; Giannozzi et al., 2009). The Perdew–Burke–Ernzerhof (PBE) functional was used for exchange-correlation energy (Perdew et al., 1998) alongside norm-conserving pseudopotentials (Troullier & Martins, 1991). A kinetic energy cut-off of 70 Ry for wave functions and 700 Ry for charge density was applied with an 8 × 8 × 8 Monkhorst–Pack k-point grid (Monkhorst & Pack, 1976). Ionic positions and lattice parameters were optimized using the BFGS algorithm (Broyden, 1970). Phonon dispersion and density of states were computed using density functional perturbation theory (DFPT) (Baroni et al., 2001b). On a 4 × 4 × 4 q-point mesh. Elastic constants were derived using the thermo_pw code (Corso, 2016). And optical properties were calculated with time-dependent density functional theory (TDDFT) via the turbo_eels package (Motornyi et al., 2020; Timrov et al., 2015a; Timrov et al., 2015b).

Results and Discussion

Table 1. Structural, electronic and elastic properties

Structural and electronic properties		a (A)	B (GPa)	B'	E_g^d,Eg^i
	This study	7.36	25.05	4.02	1.30, 1.35
	Other	7.65[a] 7.36[b]			2.06[c], 2.03[c]
Elastic properties		C_{11}, $C_{12,}$ C_{44}	E(GPa)	G (GPa)	υ
	This study	48.13, 12 .19, 11.19	34.22	13.54	0.26

[a](Gruhn, 2010), [b](Carrete et al., 2014), [c](Zhang et al., 2012)

Structural Properties

Half-Heusler XYZ alloys exhibit a C1b structure, classified in space group F–43m (No.: 216), with three configurations for X, Y, and Z elements: type-α, type-β, and type-γ. In the type-α phase, X occupies 4c (0.25, 0.25, 0.25), Y is at 4a (0.0, 0.0, 0.0), and Z at 4b (0.5, 0.5, 0.5). For type-β, X is at 4a, Y at 4b, and Z at 4c, while type-γ positions reverse accordingly. Energy minimization revealed the type-β phase as the most stable for KBaP, based on the total energy vs. volume curve as shown in Figure 1. The structural parameters, summarized in Table 1, were derived from Murnaghan's equation of state (Murnaghan, 1944), and align with earlier theoretical studies.

Lattice Dynamical Properties

To assess the dynamical stability of KBaP in its β-phase, we generated the phonon dispersion spectrum along high-symmetry directions, as shown in Figure 2. The absence of imaginary modes at high-symmetry k-points confirms the material's dynamical stability. This analysis is novel for KBaP. The primitive cell consists of three atoms, resulting in nine vibrational branches: three acoustic and six optical modes. Figure 2 illustrates the phonon spectrum, revealing three distinct band groups. The acoustic-optical band gap is observed at 25 cm^{-1} at the L point, attributed to variations in atomic masses.

Elastic Structure

The analysis of elastic constants is crucial for evaluating the mechanical properties of materials, including stability and ductility. For cubic structures, three independent elastic constants C11, C12, and C44 are essential,

with our calculated values summarized in Table 2. The Half-Heusler alloys meet the Born-Huang criteria for mechanical stability, and C12 being lower than C11 indicates stronger bonding in the 100 direction. Mechanical parameters like shear modulus (G), Young's modulus (E), and Poisson's ratio (ν) are estimated from these constants, with results compiled in Table 1. The B/G ratio, or Pugh's ratio, indicates ductility, as values above 1.75 suggest ductile behavior; our results show KBaP is ductile. Additionally, KBaP displays high rigidity, evident from its Young's modulus values.

The analysis of elastic constants is essential for understanding key mechanical properties such as stability, hardness, strength, stiffness, and whether materials are brittle or ductile. For cubic structures, only three independent elastic constants are relevant: C11, C12, and C44. The values we calculated for these constants, summarized in Table 2, show that the three studied Half-Heusler alloys satisfy the Born-Huang criteria for mechanical stability, specifically:

$(C_{11} + 2C_{12})/3 > 0$, $(C_{11} - C_{12})/2 > 0$, $C_{44} > 0$ and $C_{12} < B < C_{11}$ Additionally, the fact that C12 is lower than C11 implies that bonding strength is greater in the ⟨100⟩ direction than in the ⟨011⟩ direction.

Using the Voigt (V), Reuss (R), and averaged Hill approximations , we can estimate mechanical parameters such as bulk modulus B, shear modulus G, Young's modulus E, and Poisson's ratio ν from the results of the elastic constants using the following relations. (Reuss,1929;Hill, 1952).

$$B_V = B_R = \frac{C_{11}+2C_{12}}{3} \quad (1)$$

$$B_H = \frac{B_V+B_R}{2} = \frac{C_{11}+2C_{12}}{3} \quad (2)$$

$$G_V = \frac{C_{11}-C_{12}+3C_{44}}{5} \quad (3)$$

$$G_R = \frac{5G_{44}(C_{11}-C_{12})}{4C_{44}+3(C_{11}-C_{12})} \quad (4)$$

$$G_H = \frac{G_V+G_R}{2} \quad (5)$$

$$E_H = \frac{9BG}{3B+G} \quad (6)$$

$$\upsilon = \frac{3B-2G}{6B-2G} \quad (7)$$

The calculated mechanical parameters are presented in Table 1. The assessment of whether a material is brittle or ductile is typically conducted using the ratio of bulk modulus (B) to shear modulus (G), known as Pugh's ratio. According to this criterion, a B/G ratio greater than 1.75 indicates a ductile material, while a ratio below 1.75 suggests brittleness. As indicated in Table 1, all calculated B/G ratios for the compound exceed 1.75, confirming its ductile nature. Young's modulus (E), an important parameter in industrial applications, is defined as the ratio of stress to strain, which reflects the stiffness of the material; higher values of E are associated with increased stiffness. For the Half-Heusler alloy KBaP, the Young's modulus is particularly high, showcasing its significant rigidity.

Electronic Properties

The analysis of electronic band structures is essential for understanding the physical characteristics of solid material, which largely account for their optical and transport properties. Figure 3 illustrates the electronic structure along high-symmetry directions in k-space, with the Fermi level adjusted to zero. The maximum of the valence band and the minimum of the conduction band are located at the X point, indicating semiconductor behavior characterized by a direct bandgap. The bandgap energy value (Eg) for KBaP is approximately 1.30 eV. Table 1 summarizes the calculated band energie for this alloy alongside other computed values.

Optical Properties

In this section, we examine the optical properties of KBaP to evaluate its potential for use in optoelectronic devices. The optical parameters are derived from the complex dielectric function, $\epsilon(\omega)=\epsilon_1(\omega)+i\epsilon_2(\omega)$ (Pourghazi & Dadsetani, 2005) Where the imaginary part $\epsilon_2(\omega)$ represents light absorption, and the real part $\epsilon_1(\omega)$ describes the slowing down of light within the material. The dielectric function for the studied structures is illustrated in Figure 4.

At first glance, the dielectric functions of KBaP appear quite similar. From Figure 4(a), we observe that the static value of the real part $\epsilon_1(0)$ is approximately 5.75. The inverse relationship between the bandgap Eg and $\epsilon_1(0)$ supports the correlation described by the Penn model (Penn, 1962).

$$\epsilon_1(0)=\hbar\omega/Eg \tag{8}$$

The dielectric functions show a peak at 2.70 eV, located within the visible spectrum. Additionally, the real part $\epsilon 1$ becomes negative in the energy range of 4 to 11 eV, indicating metallic behavior within this energy range. The imaginary part ϵ_2, illustrated in Figure 4(b), exhibits a notable peak around 4.05 eV in the visible region, followed by a rapid decrease with small peaks also present in the UV range.

Other optical properties, including the refractive index n, extinction coefficient k, reflectivity R, and energy loss function L, can be derived from the real and imaginary parts of the dielectric function. The equations for these parameters are as follows:

$$n(\omega) = \frac{1}{\sqrt{2}}\left(\sqrt{\epsilon_1^{\,2}(\omega)+\epsilon_2^{\,2}(\omega)}+\epsilon_1(\omega)\right)^{\frac{1}{2}} \tag{9}$$

$$k(\omega) = \frac{1}{\sqrt{2}}\left(\sqrt{\epsilon_1^{\,2}(\omega)+\epsilon_2^{\,2}(\omega)}-\epsilon_1(\omega)\right)^{\frac{1}{2}} \tag{10}$$

$$R(\omega) = \frac{(n-1)^2+k^2}{(n+1)^2-k^2} \tag{11}$$

$$L(\omega) = \frac{\epsilon_2(\omega)}{\epsilon_1^{\,2}(\omega)+\epsilon_2^{\,2}(\omega)} \tag{12}$$

Figure 5(a) shows the refractive indices of the materials under investigation. n(ω) reaches a maximum in the visible region, with a maximum of 2.85 eV for KBaP. The zero-frequency refractive index n(0) is 2.40, confirming the relationship between the real part and the static refractive index $\sqrt{\epsilon_1(0)} = n(0)$.

Figure 5(b) presents the extinction coefficient as a function of photon energy. The extinction coefficient is notably low in the energy ranges below 0.85 eV and above 13.87 eV, indicating minimal light absorption, which is advantageous for the material's transparency in these energy ranges. The reflection coefficient R(ω) quantifies a material's ability to reflect electromagnetic radiation. The reflectivity graph of KBaP is shown in Figure 5(c), where the initial value is 0.17, reaching a peak at 4.20 eV, corresponding to the ultraviolet (UV) region of the alloy. Consequently, KBaP exhibit low reflectivity in the infrared and visible ranges while showing high reflectivity in the UV range, making them suitable for UV radiation protection.

The energy loss function L(ω) describes the energy lost by a fast electron traveling through a material. Figure 5(d) illustrates this energy loss function with peak values at 11.72 eV, associated with plasmon excitations. Additionally, the absorption coefficient α(ω), a key parameter for understanding light interaction with a material, can be expressed as follows (Kocak et al., 2013; Kara-Zaitri et al., 2022):

$$\alpha(\omega) = \frac{2\omega}{c}\left(\frac{1}{\sqrt{2}}\sqrt{\epsilon_1^{\,2}(\omega)+\epsilon_2^{\,2}(\omega)}-\epsilon_1(\omega)\right)^{\frac{1}{2}} \tag{13}$$

c is the speed of light in a vacuum.

Figure 6 illustrates the absorption spectrum variation as a function of the wavelength for KBaP. The proposed structure's absorption spectrum spans from 41.5 to 1000 nm. The main absorption spectrum of the studied alloy is located in the UV range, with a maximum recorded at 173 nm. KBaP exhibits the highest absorption with a maximum absorption coefficient reaching 130×10^{-4} cm^{-1} at a wavelength of 173 nm. Additionally, the

absorption coefficient approaches zero in the near-infrared range. This simulation allows for optimization of the material's absorption coefficient.

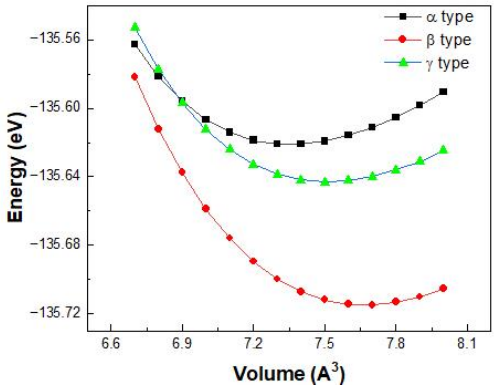

Figure 1. Energy vs Volume

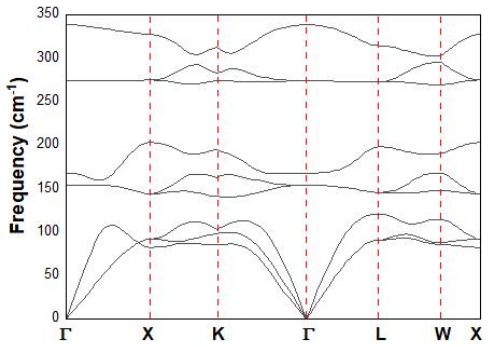

Figure 2. Phonon dispersion spectrum for KBaP

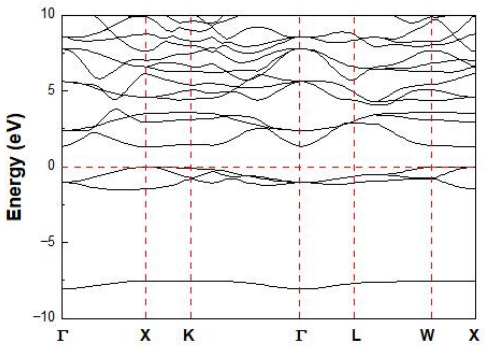

Figure 3. Band structure for KBaP

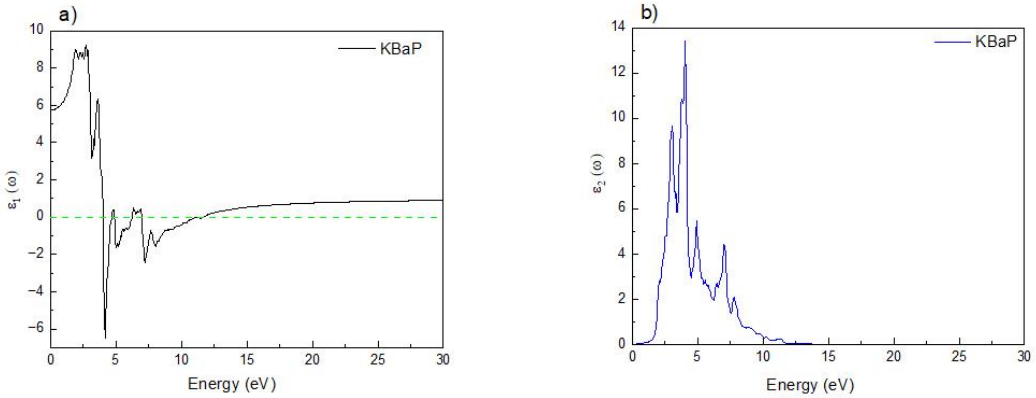

Figure 4. The dielectric function for KBaP

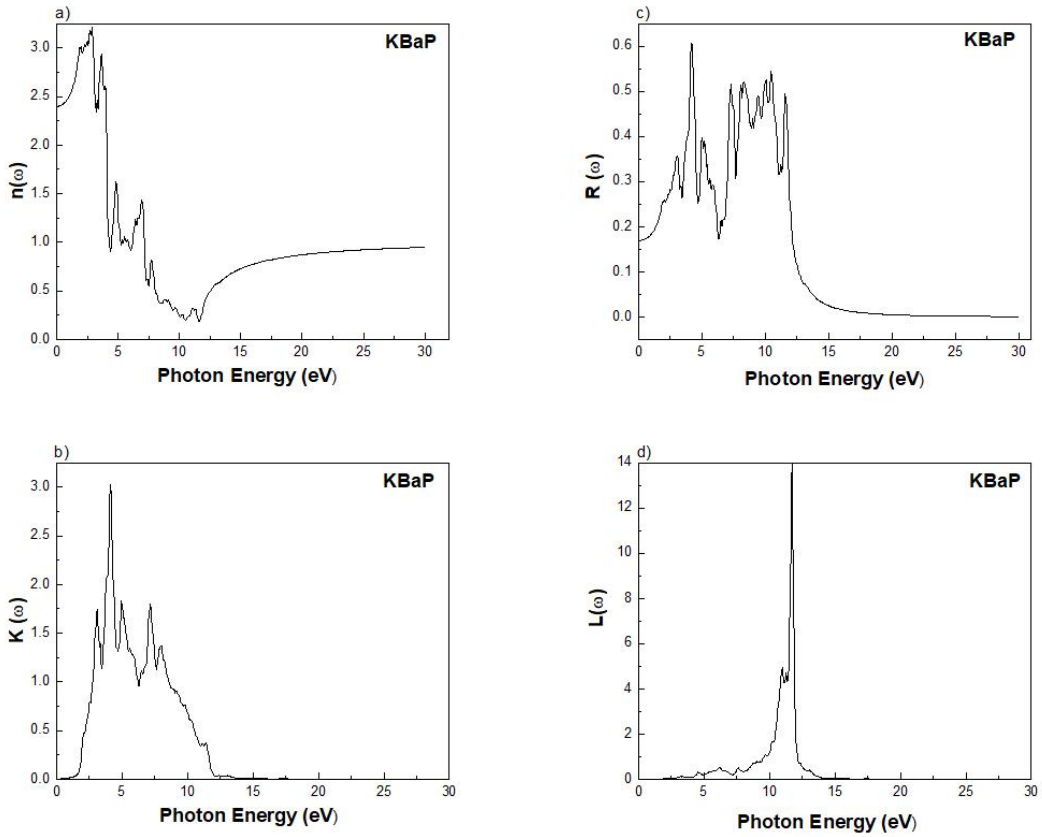

Figure 5. Optical properties for KBaP

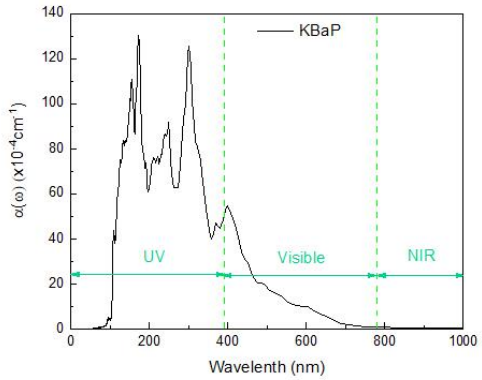

Figure 6. Absorption spectra for KBaP

Conclusion

In conclusion, this study offers a comprehensive analysis of the half-Heusler compound KBaP, providing new insights into its structural, mechanical, electronic, thermodynamic, and optical properties. Through the application of advanced computational techniques, including density functional theory (DFT) and density functional perturbation theory (DFPT), the stability of KBaP in its β-phase has been confirmed. The material exhibits promising characteristics, such as a direct bandgap of 1.30 eV, dynamic stability, and favorable elastic properties, making it a strong candidate for use in thermoelectric and optoelectronic applications. Additionally, the calculated optical properties, including the dielectric function and absorption spectra, further highlight the material's potential in ultraviolet radiation protection and other high-frequency applications. This work paves the way for future experimental studies and the exploration of KBaP's practical applications in advanced technological fields.

Scientific Ethics Declaration

The authors declares that the scientific ethical and legal responsibility of this article published in EPSTEM Journal belongs to the authors.

Acknowledgements or Notes

* This article was presented as a poster presentation at the International Conference on Technology, Engineering and Science (www.icontes.net) held in Antalya/Turkey on November 14-17, 2024.

References

Baroni, S., De Gironcoli, S., Dal Corso, A., & Giannozzi, P. (2001a). Phonons and related crystal properties from density-functional perturbation theory. *Reviews of Modern Physics*, *73*(2), 515–562.

Baroni, S., De Gironcoli, S., Dal Corso, A., & Giannozzi, P. (2001b). Phonons and related crystal properties from density-functional perturbation theory. *Reviews of Modern Physics*, *73*(2), 515–562.

Broyden, C. G. (1970). The convergence of a class of double-rank minimization algorithms 1. general considerations. *IMA Journal of Applied Mathematics*, *6*(1), 76–90.

Carrete, J., Li, W., Mingo, N., Wang, S., & Curtarolo, S. (2014). Finding unprecedentedly low-thermal-conductivity half-Heusler semiconductors via high-throughput materials modeling. *Physical Review X*, *4*(1), 011019.

Corso, A. D. (2016). Elastic constants of beryllium: A first-principles investigation. *Journal of Physics: Condensed Matter*, *28*(7), 075401.

Felser, C., & Hirohata, A. (2015). *Heusler alloys* (Vol. 222). Springer.

Felser, C., & Hirohata, A. (2016). *Heusler alloys: Properties, growth, applications* (Vol. 222). Springer.

Giannozzi, P., Andreussi, O., Brumme, T., Bunau, O., Nardelli, M. B., Calandra, M., Car, R., Cavazzoni, C., Ceresoli, D., & Cococcioni, M. (2017). Advanced capabilities for materials modelling with quantum espresso. *Journal of Physics: Condensed Matter*, *29*(46), 465901.

Giannozzi, P., Baroni, S., Bonini, N., Calandra, M., Car, R., Cavazzoni, C., Ceresoli, D., Chiarotti, G. L., Cococcioni, M., Dabo, I., Corso, A. D., Gironcoli, S. de, Fabris, S., Fratesi, G., Gebauer, R., Gerstmann, U., Gougoussis, C., Kokalj, A., Lazzeri, M., … & Wentzcovitch, R. M. (2009). Quantum espresso: A modular and open-source software project for quantum simulations of materials. *Journal of Physics: Condensed Matter*, *21*(39), 395502.

Giannozzi, P., Baseggio, O., Bonfà, P., Brunato, D., Car, R., Carnimeo, I., Cavazzoni, C., De Gironcoli, S., Delugas, P., & Ferrari Ruffino, F. (2020). Quantum espresso toward the exascale. *The Journal of Chemical Physics*, *152*(15), 154105.

Graf, T., Felser, C., & Parkin, S. S. P. (2016). Heusler compounds: Applications in spintronics. In Y. Xu, D. D. Awschalom, J. Nitta (Eds.), *Handbook of spintronics* (pp.335–364). Netherlands: Springer.

Gruhn, T. (2010). Comparative *ab initio* study of half-Heusler compounds for optoelectronic applications. *Physical Review B*, *82*(12), 125210.

Hayashi, K., Li, H., Eguchi, M., Nagashima, Y., & Miyazaki, Y. (2020). Magnetic full-Heusler compounds for thermoelectric applications. In *Magnetic materials and magnetic levitation* (Vol.65). IntechOpen

He, K., Ma, X., Chen, X., & Xue, Q. K. (2013). New materials. In M. Franz & L. Molenkamp (Eds.), *Contemporary Concepts of Condensed Matter Science* (Vol. 6, pp. 237–262). Elsevier.

Heusler, F. (1903). Uber magnetische manganlegierungen. In *Verhandlungen der Deutschen Physikalischen Gesellschaft.* (p.131). Friedr. Vieweg & Sohn.

Hill, R. (1952). The elastic behaviour of a crystalline aggregate. *Proceedings of the Physical Society Section A*, *65*(5), 349.

Hohenberg, P., & Kohn, W. (1964). Density functional theory (DFT). *Physical Review Journals*, *136*(1964), B864.

Kara-Zaitri, K., Bendaoudi, L., Ould-Mohamed, M., & Ouahrani, T. (2022). Stability and opto-electronic properties of low dimensional Ag2WS4 material, from ab initio calculations. *Materials Science in Semiconductor Processing*, *150*, 106938.

Kocak, B., Ciftci, Y. O., Colakoglu, K., Deligoz, E., & Tatar, A. (2013). Pressure depended elastic, vibration and optical properties of NbIrSn from first principles calculations. *Materials Science and Technology*, *29*(8), 925–930.

Kohn, W., & Sham, L. J. (1965). Self-Consistent equations including exchange and correlation effects. *Physical Review*, *140*(4A), A1133–A1138.

Monkhorst, H. J., & Pack, J. D. (1976). Special points for Brillouin-zone integrations. *Physical Review B, 13*(12), 5188–5192.

Motornyi, O., Vast, N., Timrov, I., Baseggio, O., Baroni, S., & Dal - Corso, A. (2020). Electron energy loss spectroscopy of bulk gold with ultrasoft pseudopotentials and the Liouville-Lanczos method. *Physical Review B, 102*(3), 035156.

Murnaghan, F. D. (1944). The compressibility of media under extreme pressures. *Proceedings of the National Academy of Sciences*, *30*(9), 244–247.

Penn, D. R. (1962). Wave-number-dependent dielectric function of semiconductors. *Physical Review*, *128*(5), 2093–2097.

Perdew, J. P., Burke, K., & Ernzerhof, M. (1998). Perdew, Burke, and Ernzerhof reply. *Physical Review Letters*, *80*(4), 891–891.

Pourghazi, A., & Dadsetani, M. (2005). Electronic and optical properties of BaTe, BaSe and BaS from first principles. *Physica B: Condensed Matter*, *370*(1–4), 35–45.

Reuss, Ajzj. (1929). Berechnung der fließgrenze von mischkristallen aufgrund der Konstanten des einkristalls. zeit. *Angewandante Mathematik und Mechanik*, *9*, 49–58.

Tavares, S., Yang, K., & Meyers, M. A. (2023). Heusler alloys: Past, properties, new alloys, and prospects. *Progress in Materials Science*, *132*, 101017.

Timrov, I., Vast, N., Gebauer, R., & Baroni, S. (2015a). Erratum: Electron energy loss and inelastic x-ray scattering cross sections from time-dependent density-functional perturbation theory. *Physical Review B, 91*(13), 139901.

Timrov, I., Vast, N., Gebauer, R., & Baroni, S. (2015b). TurboEELS—A code for the simulation of the electron energy loss and inelastic x-ray scattering spectra using the Liouville–Lanczos approach to time-dependent density-functional perturbation theory. *Computer Physics Communications*, *196*, 460–469.

Troullier, N., & Martins, J. L. (1991). Efficient pseudopotentials for plane-wave calculations. *Physical Review B, 43*(3), 1993–2006.

Wederni, A., Daza, J., Ben Mbarek, W., Saurina, J., Escoda, L., & Suñol, J.-J. (2024). Crystal structure and properties of Heusler alloys: a comprehensive review. *Metals*, *14*(6), 688.

Zhang, X., Yu, L., Zakutayev, A., & Zunger, A. (2012). Sorting stable versus unstable hypothetical compounds: the case of multi-functional abx half-Heusler filled tetrahedral structures. *Advanced Functional Materials*, *22*(7), 1425–1435.

Author Information

Aidouni Ahmed Amine
University of Ahmed Draya, Adrar, Algeria
VPR7+89M, National Road No. 06, Adrar, Algeria
Contact e-mail: *aa.aidouni@univ-adrar.edu.dz*

Ould-Mohamed Mounir
Name of Institution or University
BP 270 Blida 09000, Algeria

Aissat Abdelkader
University of Ahmed Draya, Adrar, Algeria
VPR7+89M, National Road No. 06, Adrar, Algeria

Belbachir Souheil
University Abdelhamid Bn Badis of Mostaganem, Algeria
National Road No. 11, Kharouba, Mostaganem 27000, Algeria

To cite this article:

Amine, A.A., & Mounir, O.M.., Abdelkader, A., & Souheil, B. (2024). Comprehensive investigation of structural, electronic and optical properties of KBaP using density functional theory. *The Eurasia Proceedings of Science, Technology, Engineering & Mathematics (EPSTEM), 32*, 123-130.